Chapter II.16

Accelerators for medical and industrial applications

Erik Van Der Kraaij, Wiel Kleeven
Ion Beam Applications SA (IBA), Louvain-La-Neuve, Belgium

Classical, isochronous, and synchro-cyclotrons are introduced. Transverse and longitudinal beam dynamics in these accelerators are covered. The problem of vertical focusing and isochronism in compact isochronous cyclotrons is treated in some detail. Different methods for isochronization of the cyclotron magnetic field are discussed. Typical features of the synchro-cyclotron, such as the beam capture problem, stable phase motion, and the extraction problem are discussed. The main design goals for beam injection are explained and special problems related to a central region with an internal ion source are considered. The principle of a Penning ion gauge source is addressed. The issue of vertical focusing in the cyclotron centre is briefly discussed. Several examples of numerical simulations are given. Different methods of (axial) injection are briefly outlined. Different solutions for beam extraction are described. Finally, the Rhodotron, an electron accelerator, is briefly discussed.

There are different types of accelerators for medical and industrial applications. Electrostatic and linacs are the simplest types and are the most commonly used. For example, as of 2017 there are more than 14 000 electron linacs around the world in use for cancer treatment. And in industry, there are more than 11 000 electrostatic accelerators in use for ion implantation. Reference [1] gives an overview of the wide range of applications of particle accelerators, covering the medical sector, industry and more.

The requirements of certain applications make that it is sometimes more suitable to use larger and more complex accelerators. Certain cancers for example can be better treated with proton or ion beams. Their complexity and price however make that as of today there are only approximately 100 cyclotrons and synchrotrons in use for these treatments. Proton linacs are under development for cancer treatment. In this chapter we will cover in depth the cyclotrons.

For electron beams at high energy and high intensity, the requirements again make that a different machine is sometimes more suitable than linacs. The Rhodotron is such an accelerator. Developed for industrial applications, it has recently been adapted to also function for medical isotope production. A small section at the end of this chapter is dedicated to the Rhodotron.

II.16.1 Cyclotrons

Consider a particle with charge q and mass m that moves with constant velocity v in a uniform magnetic field B. Such a particle moves in a circle with radius r; the centripetal force is provided by the Lorentz

This chapter should be cited as: Accelerators for medical and industrial applications, E. Van Der Kraaij and W. Kleeven, DOI: 10.23730/CYRSP-2024-003.1817, in: Proceedings of the Joint Universities Accelerator School (JUAS): Courses and exercises, E. Métral (ed.),
CERN Yellow Reports: School Proceedings, CERN-2024-003, DOI: 10.23730/CYRSP-2024-003, p. 1817.
© CERN, 2024. Published by CERN under the Creative Commons Attribution 4.0 license.

force acting on the particle

$$\frac{mv^2}{r} = qvB \;\Rightarrow \omega = \frac{v}{r} = \frac{qB}{m} \,. \tag{II.16.1}$$

Thus, the angular velocity is constant: it is independent of radius, velocity, energy (in the non-relativistic limit), or time. There are a few very important consequences of this feature:

1. particles can be accelerated with an RF system that operates at constant frequency and the beam is a fully continuous wave;
2. the orbits start their path in the centre (injection) and spiral outward to the pole radius (extraction);
3. the magnetic field is constant in time;
4. the RF structure and the magnetic structure are completely integrated: the same RF structure will accelerate the beam many times (allowing for a compact, cost-effective accelerator).

The cyclotron was invented in 1932 [2]. This type (quasi-uniform magnetic field) is called the classical cyclotron. The frequency of the RF-structure and the magnetic field are related as

$$f_{\mathrm{RF}} \approx 15.2\, h\, \frac{Z}{A}\, B \,. \tag{II.16.2}$$

Here Z and A are the charge number and mass number of the particle, $h = f_{\mathrm{RF}} \,/\, f_{\mathrm{ion}}$ is the harmonic mode of the acceleration and f_{RF} is expressed in megahertz, B in tesla.

II.16.1.1 Vertical stability

In a uniform magnetic field there is no vertical focusing, the motion is meta-stable. There is thus a problem with the classical cyclotron. During acceleration, the relativistic mass increases. Therefore, the angular velocity is actually not constant but gradually decreases. Equation (II.16.1) becomes

$$\omega = \frac{qB}{m_0} \sqrt{1 - \left(\frac{v}{c}\right)^2} \,, \tag{II.16.3}$$

with m_0 the particle rest-mass and c the speed of light. A loss of synchronism occurs between the RF and the beam. Simply increasing the magnetic field with radius is not possible, because the motion then becomes vertically unstable.

II.16.1.2 First solution: the synchro-cyclotron

A solution for the vertical focusing limitations of the classical cyclotron has been introduced independently by Veksler [3] and McMillan [4]. This solution, the synchro-cyclotron, differs from the classical cyclotron, in that the magnetic field gradually decreases with radius in order to obtain weak vertical focusing

$$n = -\frac{r}{B}\frac{\mathrm{d}B}{\mathrm{d}r} \Rightarrow \; \nu_z = \sqrt{n} \,, \tag{II.16.4}$$

where ν_z is the number of vertical oscillations around the reference orbit during one turn. This is also called the vertical betatron tune. Simultaneously, the RF frequency gradually decreases with time, to compensate for the decrease in magnetic field and the increase in particle mass. This type of cyclotron brings about several important consequences:

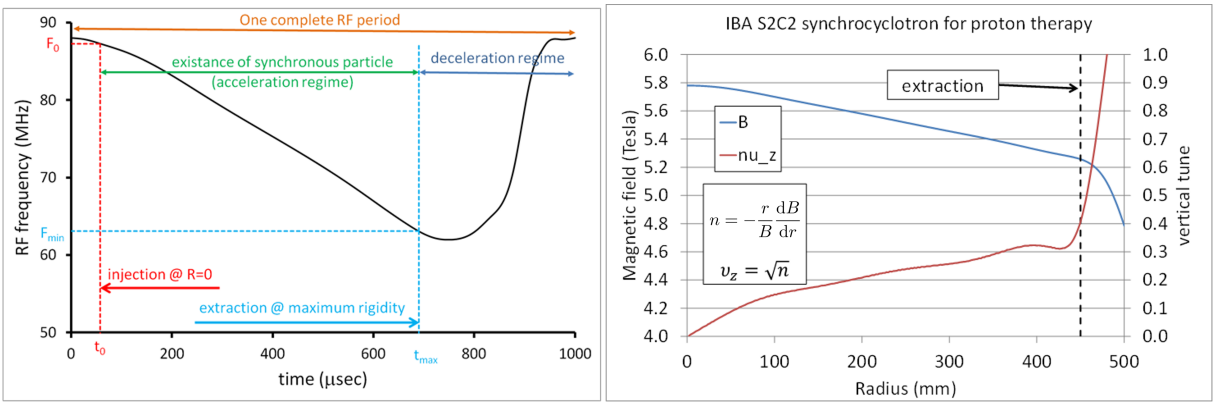

Fig. II.16.1: Properties of the IBA superconducting synchro-cyclotron (S2C2), see also text.

1. much higher energies can be obtained, in the range 100 MeV to 1 GeV;
2. the RF is pulsed but the magnetic field is constant in time (which is not the case in a synchrotron);
3. the beam is no longer continuous wave but is modulated (pulsed) in time. Thus the average beam current is much lower than for a continuous-wave machine (OK for proton therapy);
4. there is a longitudinal beam dynamics similar to that of the synchrotron;
5. the beam can only be captured in the cyclotron centre during a short time-window;
6. the timing between the RF frequency, RF voltage, and ion source needs to be well defined and controlled;
7. a more complicated (but not necessarily more expensive) RF system is needed to obtain the required frequency modulation;
8. the RF frequency cannot be varied very quickly (rotating capacitor) and therefore the acceleration must be slow. This implies the following:
   (a) low energy gain per turn;
   (b) many turns up to extraction;
   (c) low RF voltage and low RF power needed.
9. there is only a very small turn separation at extraction. Therefore a special extraction method (called a regenerative extraction) is needed to get the beam out of the machine.

Recently, IBA developed a 230 MeV superconducting synchro-cyclotron (S2C2) for proton therapy. The advantage of such a solution, as compared with compact superconducting isochronous cyclotrons, is that the average magnetic field can be increased to substantially higher values, as there is no concern about lack of vertical focusing (see later). Figure II.16.1 shows some properties of this cyclotron. The graph on the right shows the average magnetic field and the vertical focusing tune ν_z. The magnetic field in the centre is $\sim$ 5.8 T and the extraction radius is $\sim$ 450 mm; the pole radius is 500 mm. In this weak-focusing machine, the vertical focusing is produced solely by the negative field gradient. The graph on the left illustrates the time structure of the RF. The pulse length is 1 ms and the corresponding pulse rate is 1 kHz. The RF frequency varies from $\sim$ 88 MHz (when the beam is captured in the cyclotron centre) to $\sim$ 63 MHz (when the beam begins to be extracted at $r = 450$ mm). Total acceleration

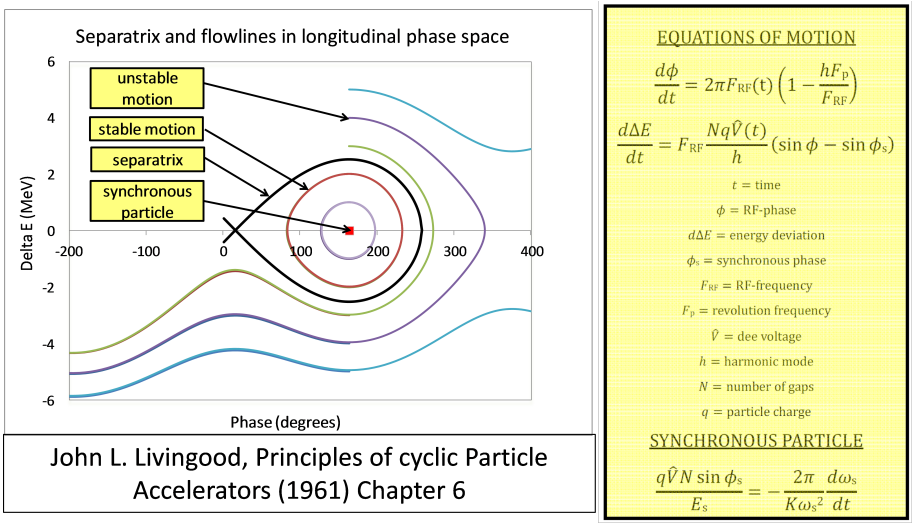

Fig. II.16.2: Longitudinal beam dynamics in a synchro-cyclotron. Left: flow lines and separatrix in longitudinal phase space. Right: equations of motion that govern this phase space.

time is ~ 600 µs, and the number of turns in this cyclotron is greater than $45\,000$.

Figure II.16.2 illustrates the longitudinal beam dynamics in the S2C2. The graph on the left shows the longitudinal phase space. For the synchronous particle, the angular velocity is (by definition) always the same as the RF frequency at all radii in the machine. A non-synchronous particle executes an oscillation around this synchronous particle. The horizontal axis is the RF phase and the vertical axis is the energy difference of the particle with respect to the synchronous particle. For small excursions, particles execute elliptical (symmetric) oscillations around the synchronous point. For larger excursions, owing to the non-linear character of the dynamics, the flow lines start to deform. The separatrix separates the stable zone from the unstable zone. Inside the separatrix, there remains, on average, a resonance between the RF frequency and the particle revolution frequency, and the particle will be accelerated. Outside the separatrix, there is no longer a resonant acceleration of the particle and it will stay close to a fixed radius in the cyclotron. The right panel of Fig. II.16.2 shows the equations of motion that govern the longitudinal phase space. More explanations of this can be found elsewhere, e.g., see Livingood [5].

II.16.1.3 Second solution: the isochronous cyclotron

In the isochronous cyclotron, an additional resource of vertical focusing is introduced by allowing the magnetic field to vary with the azimuth along a circle. This additional focusing is so strong that it dominates the vertical defocusing arising from a radially increasing field. The radial increase can be made such that the revolution frequency of the particles remains constant in the machine, even for relativistic energies (for which the mass increase is significant). This new resource of vertical focusing was invented by Thomas [6]. In the next section, this type of cyclotron is discussed in more detail.

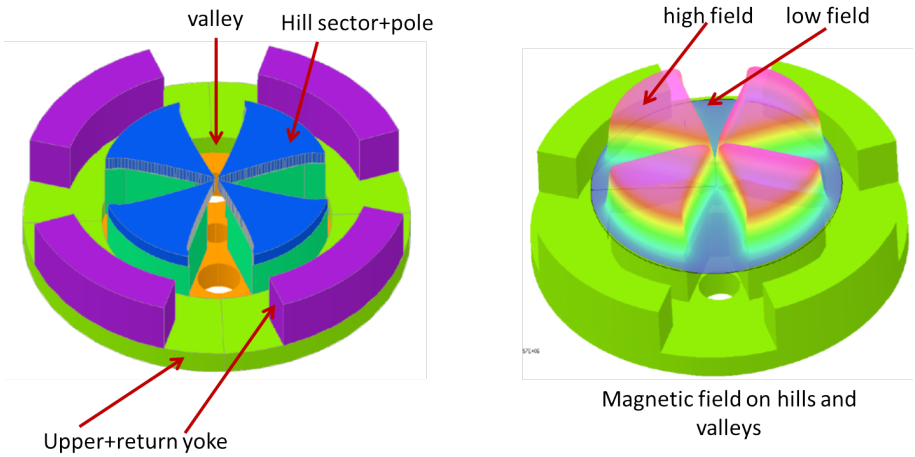

Fig. II.16.3: Magnet of a compact azimuthally varying field cyclotron. Left: the hill sectors and poles, the valleys, and the different parts of the yoke. Right: histogram of the magnetic field.

II.16.2 More about compact azimuthally varying field cyclotrons

II.16.2.1 Vertical focusing in cyclotrons

To better understand the vertical focusing in a cyclotron, consider the vertical component of the Lorentz force

$$F_z = q(\vec{v} \times \vec{B})_z = -q\left(v_\theta B_r - v_r B_\theta\right) \ . \tag{II.16.5}$$

The first term, $v_\theta B_r$, is obtained in a radially decreasing, rotationally symmetric magnetic field, such as for the classical cyclotron or the synchro-cyclotron. If only this term is present, it corresponds to the case of weak focusing. The second term, $v_r B_\theta$, requires an azimuthal modulation of the magnetic field. If such a modulation exists, it generates, by itself, also a radial component of the velocity.

The azimuthal field modulation can be produced by introducing high-field sectors (hills), separated by low-field regions (valleys). This is illustrated in Fig. II.16.3, which shows the magnet of a compact four-fold symmetrical azimuthally varying field (AVF) cyclotron with four hills and four valleys. The hill sectors are mounted on upper and lower plates of the yoke and surrounded by a return yoke placed in between the upper and lower plates. The plates contain circular holes in the valleys, which are used for vacuum pumping or installation of RF cavities. The right panel shows a histogram of the magnetic field in the median plane superimposed on the geometry. This field map was computed using the 3D finite-element software package Opera-3d from Dassault Systems [7].

Figure II.16.4 illustrates the vertical focusing in such an AVF cyclotron. The drawing on the left shows how a computed closed orbit oscillates around a reference circle to produce a scalloped orbit. The upper graph on the right shows the azimuthal component of the field in a circle 10 mm from the median plane. It can be seen that B_θ is strongly peaked at the entrance and exit of the sector. The lower graph on the right shows the (normalized) radial component of the velocity v_r. The maximum of this component is also at the entrance and exit of the sector. The product of both terms is positive at both the sector entrance and exit, indicating that the vertical focusing is concentrated at these azimuthal locations and is always positive (not alternating).

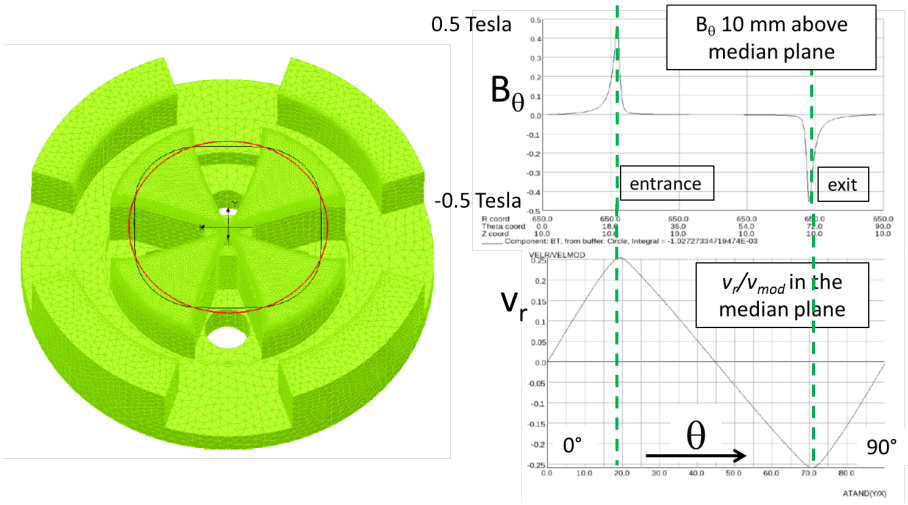

Fig. II.16.4: Vertical focusing in an azimuthally varying field cyclotron. Left: scalloping of the orbit with respect to the geometrical circle. Right: the radial velocity component and the azimuthal field component 10 mm above the median plane.

It is interesting to note that Thomas [6] invented sector focusing (Thomas focusing) in 1938, several years before the invention of the synchro-cyclotron and the synchrotron. However, his solution could not be applied immediately, owing to the increased complexity of the magnetic structure. This is why synchro-cyclotrons have been used at the birth of proton therapy.

The vertical focusing created in an AVF cyclotron can be strongly increased if the shape of the sectors is changed from straight to spiral, see Fig. II.16.5. By drawing the normal vector on the closed orbit at the sector edges, it can be seen that the angle between the orbit and the edge can be made rather large (choosing a large spiral); thus, generating a strong vertical (de-)focusing effect. However, it can also be seen that the direction of the vertical force changes sign between entrance and exit of the sector. Thus, the spiralling of the sectors creates a sequence of alternating focusing, which can become relatively strong. This strong (alternating) focusing was invented by Christofilos, Courant *et al.* [8, 9].

We note that in many compact cyclotrons, the vertical focusing is not only concentrated at the sector edges, but can be more distributed along the closed orbit:

1. edge focusing occurs at the entrance and exit of the hill sectors;
2. for spiral sectors, this focusing starts to alternate and can be made stronger;
3. in the middle of a hill sector, there can be a positive field gradient (e.g., by application of an elliptical pole gap), creating vertical defocusing;
4. in the middle of the valley, there is often a negative field gradient, creating vertical focusing.

The strength of the azimuthal field variation in a cyclotron is expressed in the flutter function F

$$F(r) = \frac{\overline{B^2} - (\,\overline{B}\,)^2}{(\,\overline{B}\,)^2}\,. \tag{II.16.6}$$

Here, $\overline{B}$ is the average of the median magnetic field over the azimuthal range from 0° to 360° and $\overline{B^2}$ is

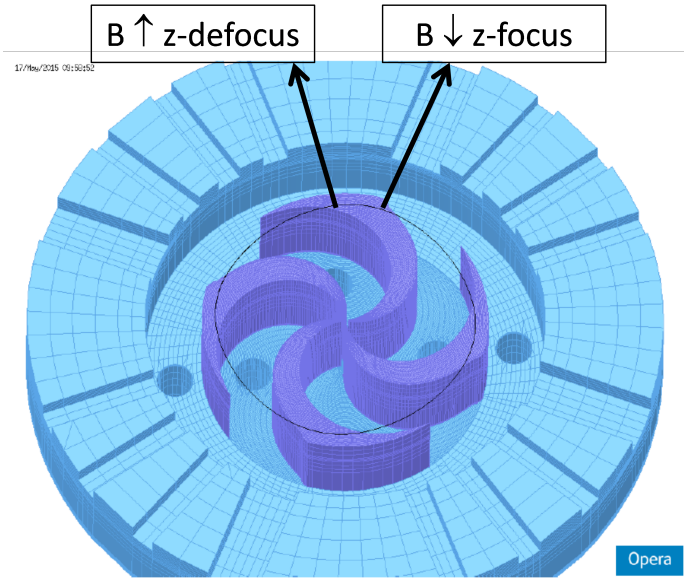

Fig. II.16.5: Vertical focusing in a cyclotron can be strongly increased by spiralling the hill sectors.

the average over the square of this field. The median plane magnetic field can be represented in a Fourier series as

$$B(r,\theta) = B(r)\left[1 + \sum_{n=1}^{\infty} A_n(r)\cos n\theta + B_n(r)\sin n\theta\right] , \tag{II.16.7}$$

where A_n and B_n are the normalized Fourier harmonics of the field. With this representation of the field, the flutter can be written as

$$F = \sum_{n=1}^{\infty} \frac{A_n^2 + B_n^2}{2} . \tag{II.16.8}$$

Often, in a compact cyclotron, a hard-edge model of the magnetic field can be used to estimate the flutter. This is illustrated in Fig. II.16.6 for a cyclotron with four-fold symmetry. The drawing on the left defines the hill angle $\alpha\pi/2$ and the valley angle $(1-\alpha)\pi/2$. The parameter α is a kind of filling factor. The drawing on the right shows the hard-edge field approximation, with B_v the field in the valley and B_h the field in the hill. The parameter N is the number of the symmetry periods in the magnet. It is easily seen that for such a model, the flutter takes the form

$$F = \alpha(1-\alpha)\left(\frac{\Delta B}{B}\right)^2 , \tag{II.16.9}$$

where $\Delta B = B_h - B_v$. Thus, the maximum flutter is obtained for $\alpha = 0.5$, where the hills and the valleys have the same width.

The flutter is a useful quantity, as the betatron oscillation tunes ν_z and ν_r can be expressed quite precisely in terms of F. Also called the vertical and radial tunings, their expressions are

$$\nu_z^2 = k \quad + \quad \frac{N^2}{N^2-1} F(1 + 2\tan^2\xi) , \tag{II.16.10}$$

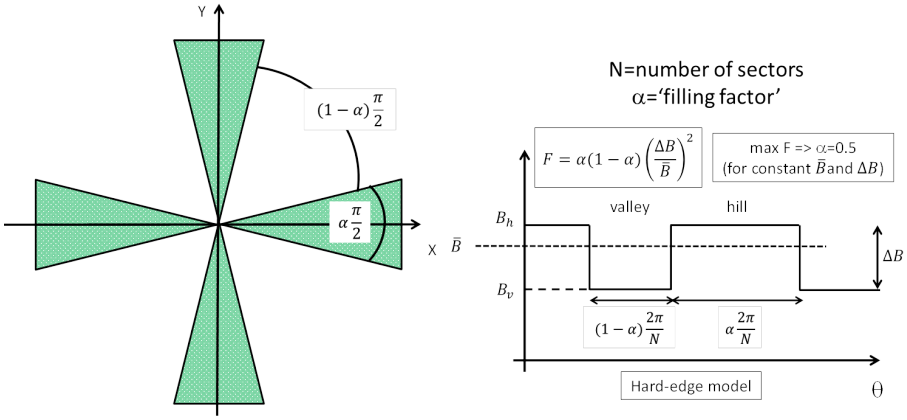

Fig. II.16.6: Simple model to estimate the flutter in a hard-edge approximation.

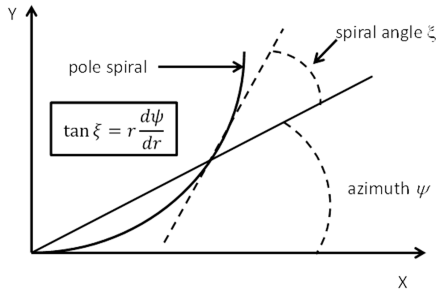

Fig. II.16.7: Spiral angle ξ of the pole.

$$\nu_r^2 = (1-k) \quad + \quad \frac{3N^2}{(N^2-1)(N^2-4)} F(1+\tan^2\xi)\,. \tag{II.16.11}$$

Here, k is the field index and ξ is the spiral angle of the pole. This angle is defined in Fig. II.16.7.

We note that Eqs. (II.16.10) and (II.16.11) are approximations. A better approximation has been obtained by Hagedoorn and Verster [10]; they express the tuning functions in terms of the Fourier components A_n and B_n of the magnetic field.

II.16.2.2 Different ways to isochronize a cyclotron

Often, cyclotrons for medical isotope production or proton therapy are fixed-field, single-particle machines. In such a case, the isochronization of the magnetic field can be achieved by shimming the iron of the pole sectors. This is illustrated in Fig. II.16.8. Each pole contains an (easily) removable pole edge that can be shimmed. For a rough estimate of the shimming δ that is needed to compensate a certain field error ΔB, a hard-edge model can be used, as illustrated in the lower left panel of Fig. II.16.8. This gives

$$\Delta\bar{B} = \frac{\delta}{2\pi}\Delta B\,, \tag{II.16.12}$$

where ΔB is the difference between the hill field and the valley field. Care must be taken that not too much iron is removed. Several iterations are often needed, with some safety margin applied each time.

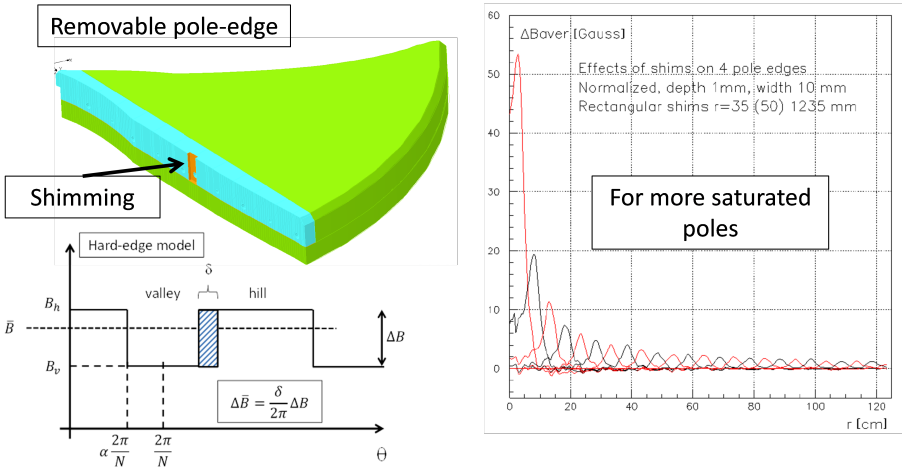

Fig. II.16.8: Upper left: isochronization of a cyclotron magnetic field is achieved by machining the profile of a removable pole edge. Lower left: a rough estimate of the shimming effect (change of the average magnetic field) can be obtained with a hard-edge model. Right: a better prediction of the shimming can be obtained by calculating (with a 3D finite-element code) the change of the radial profile of the average magnetic field due to a well-defined pole cut and repeating this for several cuts at varying radii.

A hard-edge model is not so precise and does not take into account the effect that magnetic flux is not completely removed together with the iron that has been cut, but may redistribute to radii other than where the cut was made. This may particularly occur when the iron is saturated. A better estimate can be obtained by using a 3D finite-element code to calculate the effect of a multitude of individual small shims at gradually increasing radius on the pole edge. Then, for each pole cut, the modification of the average magnetic field as a function of radius is obtained. This is illustrated in the right panel of Fig. II.16.8. From this, a shimming matrix is obtained, which relates the change of the average field $\Delta\bar{B}(r_1, r_2)$ at radius r_2 due to a small cut at radius r_1. Such a matrix is calculated once for a given (prototype) cyclotron and can then be used to speed up the isochronization of all following cyclotrons of the same type.

Modern cyclotrons for the production of PET isotopes can often accelerate two types of particle, namely H^- and D^- ions. For D^- ions, about half the energy of H^- ions can be obtained. The magnetic field remains fixed. However, the relativistic field correction needed for H^- ions is about four times as large as for D^- ions. Thus, two different isochronous field maps need to be made in the machine. In some IBA cyclotrons, this is done with the so-called 'flaps'; these are movable iron wedges that are placed in two opposite valleys in the cyclotron. For the H^- ion field, the flaps are moved vertically to a position close to the median plane. In this configuration, the average magnetic field increases approximately 2% (for the IBA C18/9 cyclotron) in order to create the H^- isochronous field shape. For D^- ions, the flaps are moved farther away from the median plane, such that their contribution to the field is strongly reduced. In the cyclotron, there are still removable pole edges on the hills, which can be shimmed to create an isochronous field shape for the deuterons. The wedge shapes of the flaps are optimized, to create the isochronous field shape for the protons. This optimization needs to be done only once (for the prototype cyclotron). The geometry of the C18/9 cyclotron is shown in Fig. II.16.9, together with an illustration of both the proton and deuteron isochronous field profiles.

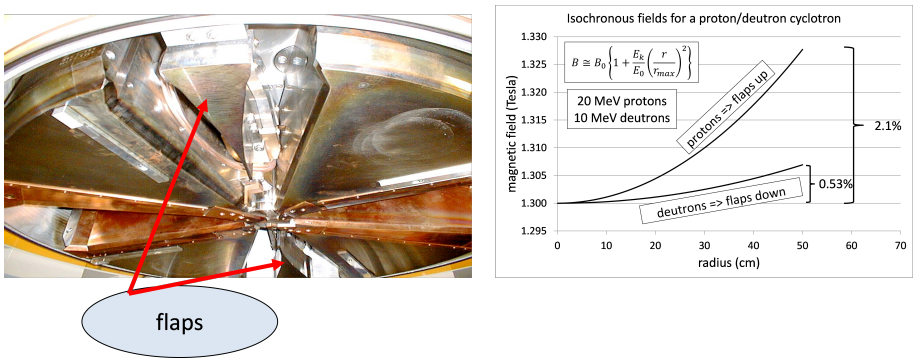

Fig. II.16.9: Left: upper poles of the IBA C18/9 cyclotron. The movable iron wedges (flaps) are used to change the average magnetic field profile from protons (flaps close to the median plane) to deuterons (flaps farther away from the median plane). Right: relativistic correction of the magnetic field, as needed for protons (about 2.1%) and for deuterons (about 0.53%).

II.16.3 Injection into a cyclotron

In this section, the main design goals for beam injection are explained and special problems related to a central region with internal ion source are considered. The principle of a PIG (Penning Ionization Gauge) source is addressed. The issue of vertical focusing in the cyclotron centre is briefly discussed. Several examples of numerical simulations are given. Axial injection is also briefly outlined.

The topic of cyclotron injection has already been covered in earlier CAS proceedings of the general accelerator physics course [11], as well as in CAS proceedings of specialized courses [12, 13]. An overview of issues related to beam transport from the ion source into the cyclotron central region has been given by Belmont at the 23rd ECPM [14].

Two fundamentally different injection approaches can be distinguished, depending on the position of the ion source. An internal ion source is placed in the centre of the cyclotron, where it constitutes an integrated part of the RF accelerating structure. This may be a trivial case, but it is the one that is most often implemented for compact industrial cyclotrons, as well as for proton therapy cyclotrons. The alternative is the use of an external ion source, where some kind of injection line with magnets for beam guiding and focusing is needed, together with some kind of inflector to kick the beam onto the equilibrium orbit. This method is used for higher-intensity isotope production cyclotrons and also in the proposed IBA C400 cyclotron for carbon therapy.

II.16.3.1 Design goals

Injection is the process of particle beam transfer from the ion source, where the particles are created, into the centre of the cyclotron, where the acceleration can start. When designing an injection system for a cyclotron, the following main design goals must be identified:

1. horizontal centring of the beam with respect to the cyclotron centre. This is equivalent to placing the beam on the correct equilibrium orbit given by the injection energy;
2. matching (if possible) of the beam phase space to the cyclotron eigenellipse (acceptance);
3. vertical centring of the beam with respect to the median plane;

4. longitudinal matching (bunching), i.e., compressing the DC beam from the ion source into shorter packages at the frequency of the RF;
5. minimization of beam losses and preservation (as much as possible) of the beam quality between the ion source and the cyclotron centre.

The requirement of centring of the beam with respect to the cyclotron centre is equivalent to requiring that the beam is well positioned on the equilibrium orbit corresponding to the energy of the injected particles. The underlying physical reasons for the first three requirements are the same. A beam that is not well centred or is badly matched will execute coherent oscillations during acceleration. In the case of off-centring, these are beam centre-of-mass oscillations. In the case of phase-space mismatch, these are beam envelope oscillations. After many turns , these coherent oscillations smear out and directly lead to an increase in the circulating beam emittances. Consequently, beam sizes will be larger, the beam is more sensitive to harmful resonance, the extraction will be more difficult, and the beam quality of the extracted beam will be lower.

The last two requirements directly relate to the efficiency of injection into the cyclotron. Longitudinal matching requires a buncher, which compresses the longitudinal DC beam coming from the ion source into RF buckets. A buncher usually contains an electrode or small cavity that oscillates at the same RF frequency as the cyclotron dees. It works like a longitudinal lens that introduces a velocity modulation of the beam. After a sufficient drift, this velocity modulation transfers into longitudinal density modulation. The goal is to obtain an RF bucket phase width smaller than the longitudinal cyclotron acceptance. For a compact cyclotron without flat-top dees, the longitudinal acceptance is usually around 10–15%. With a simple buncher, a gain of a factor of two to three can easily be obtained. However, at increasing beam intensities, the gain starts to drop, owing to longitudinal space charge forces that counteract the longitudinal density modulation.

The issue of beam loss minimization also occurs, for example, in the design of the electrodes of an axial inflector. Here, it must be ensured that the beam centroid is well centred with respect to the electrodes. This is not a trivial task, owing to the complicated 3D orbit shape in an inflector. An iterative process of 3D electric field simulation and orbit tracking is required.

II.16.3.2 Constraints

It should be kept in mind that the design of the injection system is often constrained by requirements at a higher level of full cyclotron design. Such constraints can be determined, for example by:

1. the magnetic structure, with the magnetic field value and shape in the centre. Also the space that is available for the central region, inflector, ion source, etc;
2. the accelerating structure: the number of accelerating dees, the dee voltage, the RF harmonic mode;
3. the injected particle: the charge-to-mass ratio of the particle, the number of internal ion sources to be placed (one or two), and the injection energy.

II.16.3.3 Cyclotrons with an internal ion source

The use of an internal ion source is the simplest and certainly also the least expensive solution for injection into a cyclotron. Internal ion sources are used in proton therapy cyclotrons as well as in isotope production cyclotrons. The internal ion source is also used in high-field (6–9 T) superconducting synchro-cyclotrons for proton therapy (see, for example, Ref. [15]). Besides the elimination of the injection line, a main advantage lies in the compactness of the design. This opens up the possibility of placing two ion sources in the machine simultaneously. In many small PET cyclotrons, an H^- and a D^- source are included, to be able to accelerate and extract both protons and deuterons. These two particles are sufficient to produce four well-known and frequently used PET isotopes ^{11}C, ^{13}N, ^{15}O, and ^{18}F. However, an internal ion source brings several limitations: (i) often only low to moderate beam intensities can be obtained; (ii) only simple ion species such as, for example, H^+, H^-, D^-, ^3He, or ^4He can be obtained; (iii) injected beam manipulation, such as matching or bunching is not possible; (iv) there is a direct gas leak into the cyclotron, which might be especially limiting for the acceleration of negative ions because of vacuum stripping; (v) high beam quality is more difficult to obtain; and (vi) source maintenance requires venting and opening the cyclotron.

II.16.3.3.1 The Penning ionization gauge ion source

A cold-cathode PIG [16] ion source is often used as an internal source. The PIG source contains two cathodes that are placed at each end of a cylindrical anode (see Fig. II.16.10). The cathodes are at negative potential relative to the anode (the chimney). They emit electrons that are needed to ionize the hydrogen gas and create the plasma. The cyclotron magnetic field must be along the axis of the anode. This field is essential for the functioning of the source, as it enhances confinement of the electrons in the plasma and therefore the level of ionization of the gas. The electrons oscillate up and down as they are reflected between the two cathodes and spiralize around the vertical magnetic field. To initiate the arc current, the cathode voltage must initially be raised to a few kilovolts. Once a plasma is formed, the cathodes are self-heated by ionic bombardment and the arc voltage will decrease with increasing arc current. Usually, an operating voltage of a few hundred volts is obtained. This is sufficient to ionize the gas atoms. The ions to be accelerated are extracted from the source via a small aperture called the slit. This extraction is obtained by the electric field that exists in between the chimney and the so-called puller. This puller is at the same electric potential as the RF accelerating structure, as it is mechanically connected to the dees (see Fig. II.16.11).

The right panel of Fig. II.16.10 shows chimneys and cathodes used in compact IBA cyclotrons. The chimneys are made of a copper-tungsten alloy, which has good thermal properties and good machining properties. The cathodes are fabricated from tantalum, because of its good thermal properties and its low work function for electron emission.

II.16.3.3.2 Vertical focusing in the cyclotron centre

The azimuthal field variation goes to zero in the centre of the cyclotron; therefore, this resource for vertical focusing is lacking. There are two remedies to restore the vertical focusing:

1. add a small magnetic field bump (a few hundred gauss) in the centre. The negative radial gradient

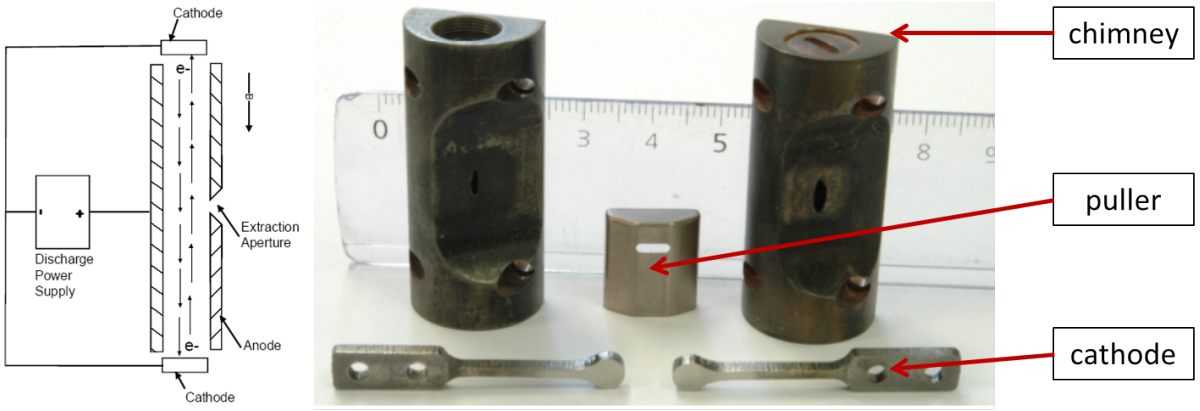

Fig. II.16.10: Left: cold-cathode Penning ion gauge source. Right: two chimneys, two cathodes, and a puller. The chimney on the right shows an eroded slit.

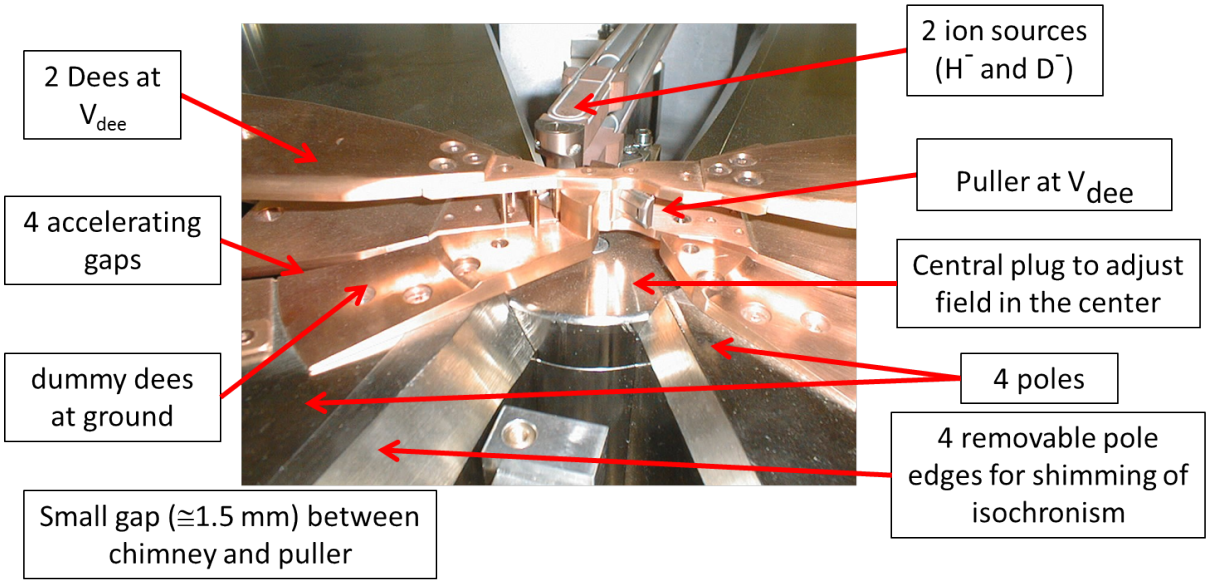

Fig. II.16.11: Central region of the IBA C18/9 cyclotron showing the dees and dummy dees. One of the two ion sources has been removed to show the puller. The figure also shows the four hill sectors. The removable circular disc underneath the central region is the central plug; it is used to fine tune the magnetic field bump in the centre.

of this bump provides some vertical focusing. The bump must not be too large, to avoid too large an RF phase slip. In small IBA PET cyclotrons, the bump is fine tuned by modifying the thickness of the central plug (see Fig. II.16.11);

2. fully exploit the electrical focusing provided by the first few accelerating gaps.

If an accelerating gap is well positioned with respect to the RF phase, it may provide some electrical focusing. Figure II.16.12 illustrates the shape of the electric field lines in the accelerating gap between a dummy dee (at ground potential) and the dee. The particle is moving from left to right and is accelerated in the gap. In the first half of the gap, the vertical forces point towards the median plane and

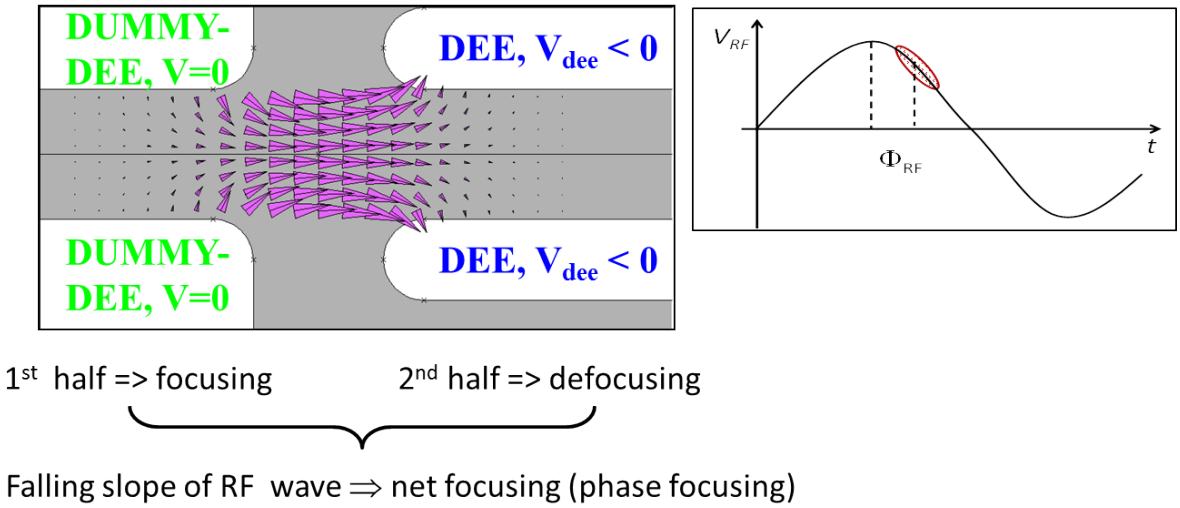

Fig. II.16.12: Vertical electrical focusing in the cyclotron accelerating gap. This focusing is important only in the cyclotron centre.

this part of the gap is vertically focusing. In the second half of the gap, the vertical forces have changed sign and this part of the gap is vertically defocusing. If the dee voltage were DC, there would already be a net focusing effect of the gap for two reasons: (a) a focusing and de-focusing lens, one behind the other, provide some net focusing in both planes and (b) the defocusing lens is weaker because the particle has a higher velocity in the second part of the gap. This is comparable to the focusing obtained in an Einzel lens. However, the dee voltage is not DC but varying in time and this may provide an additional focusing term that is more important than the previous two effects (phase focusing). This is obtained by letting the particle cross the gap at the moment that the dee voltage is falling (instead of accelerating at the top). In this case, the defocusing effect of the second gap half is additionally decreased. To achieve this, the first few accelerating gaps must be properly positioned azimuthally. This forms part of the central region design.

II.16.3.3.3 The central region of a superconducting synchro-cyclotron

The internal cold-cathode PIG ion source is also used in superconducting synchro-cyclotrons for proton therapy. In such a cyclotron, the magnetic field in the centre is very high (5–9 T) and the energy gain per turn is low, with a dee voltage of about 10 kV. In such a case, the central region needs to be very compact. This is illustrated in Fig. II.16.13, which shows the central region of the IBA S2C2. The source diameter is < 5 mm and the diameter of the first turn in the cyclotron is $\approx$6 mm. The vertical dee gap in the centre is only 6 mm. The first 100 turns are within a radius of only 30 mm.

II.16.3.4 Cyclotrons with an external ion source

In many cases, the ion source is placed outside the cyclotron. There may be different reasons for this choice: (i) higher beam intensities are needed, which can only be produced in a more complex and larger ion source than the simple PIG source, (ii) special ion species, such as heavy ions or highly stripped

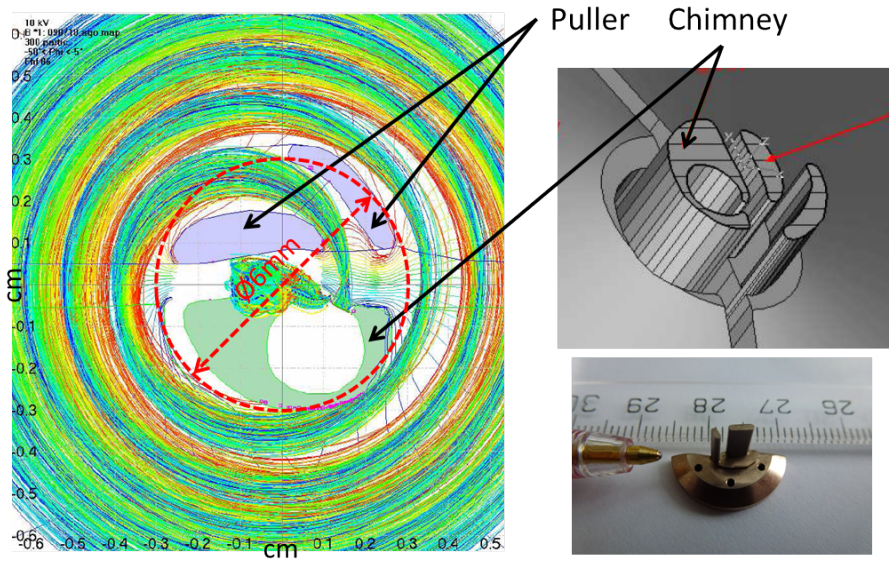

Fig. II.16.13: Left: calculated orbits in the central region of the IBA S2C2. Right: 3D view of the Penning ion gauge source and puller used in this central region.

ions, are required, or (iii) a good machine vacuum is needed (for example, H^- acceleration). External ion sources are used in high-intensity isotope production cyclotrons but, for example, also in the proposed IBA C400 cyclotron for carbon therapy. Of course, the external ion source is a more complex and more expensive solution, since it requires an injection line with all related equipment such as magnetic or electrostatic beam guiding and focusing elements, vacuum equipment, beam diagnostics, etc.

II.16.3.4.1 Inflectors for axial injection

There are a few different ways to inject into a cyclotron. Using inflectors for axial injection, the electrical field between two electrodes bends the beam 90° from vertical to horizontal. The presence of the cyclotron magnetic field creates a complicated 3D orbit; this makes the inflector design difficult.

The most common used inflector is of the spiral kind. This is a cylindrical capacitor that is gradually twisted to take into account the spiralling of the trajectory, induced by the vertical cyclotron magnetic field. By design, the electrical field is always perpendicular to the velocity vector of the central particle, positioning the orbit on an equipotential surface. The formula for the electrode voltage is

$$V = 2 \cdot \frac{E}{q} \cdot \frac{d}{R_e} \,, \tag{II.16.13}$$

where V is the electrode voltage, E is the injection energy, q is the particle charge, d is the electrode spacing, and R_e is the electric radius of the inflector (which is almost equal to the inflector height). An important advantage of the spiral inflector is that it has two free design parameters that can be used to place the particle on the correct equilibrium orbit. These two parameters are the electrical radius, R_e, and the so-called tilt parameter, k'. This second parameter represents a gradual rotation of the electrodes around the particle moving direction by which a horizontal electric field component is obtained that is

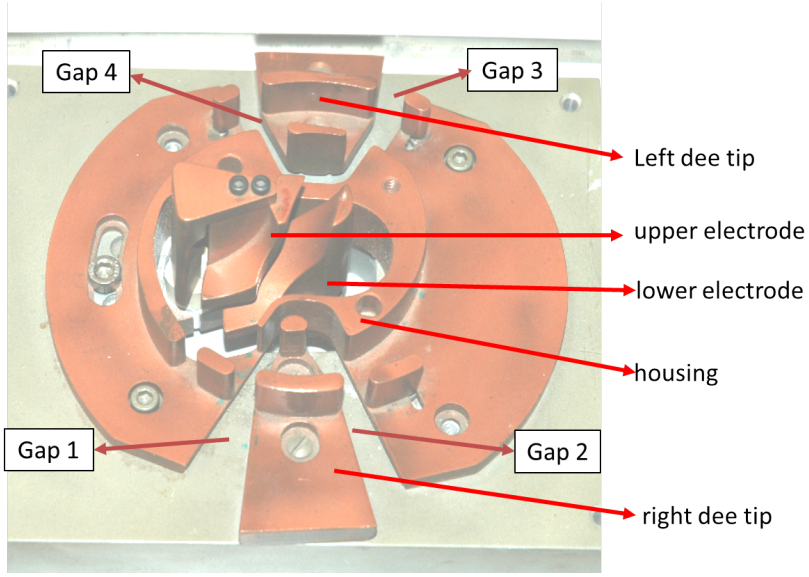

Fig. II.16.14: 1:1 model of the spiral inflector and central region of the IBA Cyclone 30 cyclotron.

proportional to the horizontal velocity component of the particle. Varying k' is, therefore, equivalent (as far as the central trajectory is concerned) to varying the cyclotron magnetic field in the inflector volume. Another advantage of the spiral inflector is its compactness. Figure II.16.14 shows a 1:1 model of the spiral inflector used in the IBA C30 cyclotron.

II.16.3.4.2 Example: axial injection in the IBA C30HC high-intensity cyclotron

Analytical formulae exist for central orbits in a spiral inflector placed in a homogeneous magnetic field, see Refs. [17–20]. However, the field in the cyclotron centre is certainly not uniform, owing to the axial hole needed for axial injection. In practice, the inflector design requires extensive numerical effort, which can be broken down into three main parts: (1) 3D modelling of the electrical fields of the inflector and central region, (2) 3D modelling of the magnetic field in the central region, and (3) orbit tracking in the central region. The complete process is tedious and requires many iterations. First, the central trajectory has to be defined and optimized. There are three main requirements, namely that the injected orbit is nicely on the equilibrium orbit, correctly placed in the median plane and well centred with respect to the inflector electrodes. After an acceptable electrode geometry has been obtained, for which these requirements are fulfilled, the beam optics must be studied. Here the main requirement is that reasonable matching into the cyclotron eigenellipse can be achieved, so that large emittance growth in the cyclotron is avoided [21].

It may be necessary to calculate several inflectors of different height, A, and tilt parameter, k', to optimize this process. At IBA, both the 3D magnetic field computations as well as the 3D electrical field computations are done using the Opera-3d software package from Dassault Systems [7]. Often, the models are completely parameterized, for quick modification and optimization. Figure II.16.15 shows such a model of the central region and the inflector. The inflector model uses the following parameters: the electrode width and spacing (both may vary along the inflector), the tilt parameter k', and the shape

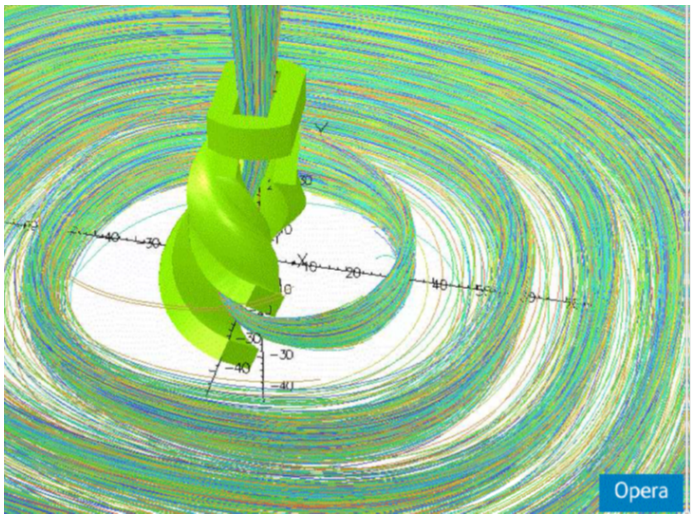

Fig. II.16.15: Left: axially injected 3D orbits calculated with the cyclotron tracking code AOC are imported in the Opera-3d finite-element model of the IBA C30XP cyclotron. Right: central region of the IBA C70XP cyclotron, showing the inflector with an additional electrode at its exit that provides a radial kick, which is needed to centre particles with different q/m ratios on their respective equilibrium orbits.

of the central trajectory itself, in terms of a list of points and velocity vectors.

II.16.4 Extraction from cyclotrons

Extraction is the process of beam transfer from an internal orbit to a target that is placed outside of the magnetic field. There are two main reasons why extraction is considered as difficult:

1. in a cyclotron, the turn separation is inversely proportional to the radius ($R \approx \sqrt{E}$). Because of this, the turns pile up closely together near the extraction radius. Therefore, it is difficult to deflect the last orbit, without influencing the inner orbits and without important beam losses;
2. during extraction, the beam has to cross the fringe field. This is an area where there are very large gradients and non-linearities in the magnetic field. Special precautions have to be made to avoid substantial beam losses, beam blow-up, or loss of beam quality.

There are a few different ways to solve the problem of extraction:

1. no extraction at all: avoid the problem by using an internal target. This can be done for isotope production, but is a little bit dirty;
2. extraction by stripping (H^- or H_2^+ cyclotrons), often applied in isotope production cyclotrons;
3. use one (or more) electrostatic deflectors (ESDs) that peel off the last orbit: this is, for example, done in the proton therapy cyclotrons of Varian, IBA, and SHI;
4. regenerative extraction, as used in synchro-cyclotrons: this is, for example, done in the proton therapy synchro-cyclotrons of Mevion and IBA;
5. self-extraction: this requires a suitable and precise shaping of the magnetic field. IBA has made one such prototype cyclotron for isotope production.

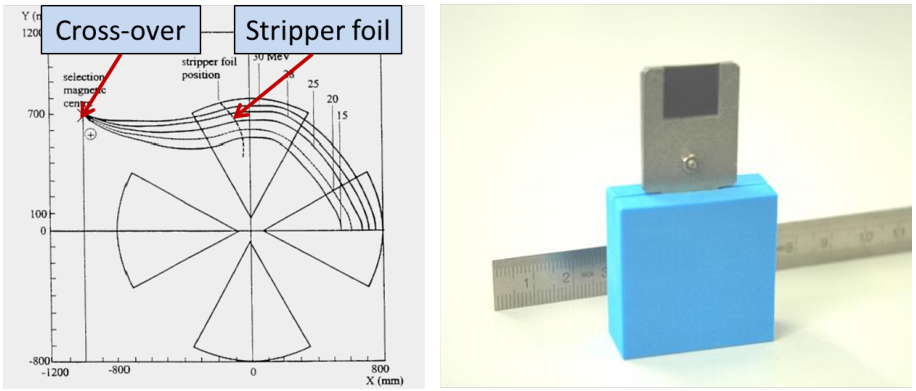

Fig. II.16.16: Left: H^- extraction by stripping. Energy is selected by moving the stripper foil to the correct radius. Right: a simple carbon stripper foil is used to extract the beam (typically 50–200 $\mu g/cm^2$).

Cases (2) and (3) require some method to increase the turn separation between the last and penultimate orbits. Different solutions for beam extraction are now treated: by stripping, by using a deflector, and the regenerative extraction used in synchro-cyclotrons. Note that this topic has been covered in more detail in earlier courses, see Refs. [11, 13, 22].

II.16.4.1 Stripping extraction

To extract the beam, the particles pass a thin stripper foil (see the right panel of Fig. II.16.16), by which one or more electrons are removed from the ion. Because of this, there is an instantaneous change of the orbit local radius of curvature. The relation between the local radius before (ρ_i) and after (ρ_f) stripping is given by

$$\rho_f = \frac{Z_i}{Z_f}\frac{M_f}{M_i}\rho_i \,, \tag{II.16.14}$$

where M_i and M_f are the particle mass before and after stripping, respectively. As an example, for H^-, we have $H^- \Rightarrow H^+ + 2e^-$ and the local radius of curvature practically only changes sign ($\rho_f = -\rho_i$) because $M_{H^+} \simeq M_{H^-}$. As a result, the stripped particle is immediately deflected outward, away from the cyclotron centre. This is illustrated in the left panel of Fig. II.16.16.

Multiple targets can be placed around the machine. This is illustrated in the left panel of Fig. II.16.17. A given target is selected by rotating the corresponding stripper foil into the beam. H^- extraction is applied in many commercial isotope production cyclotrons, fabricated, for example, by IBA (Cyclone IKON, Kiube or Key), Advanced Cyclotron Systems (TR30, TR13), or General Electric (PETtrace). The right panel of Fig. II.16.17 shows a view on the median plane of a typical IBA isotope production cyclotron. In this cyclotron, eight different target ports are available.

The most important features and advantages of stripping extraction are:

1. very simple extraction device;
2. 100% extraction efficiency;
3. variable energy;

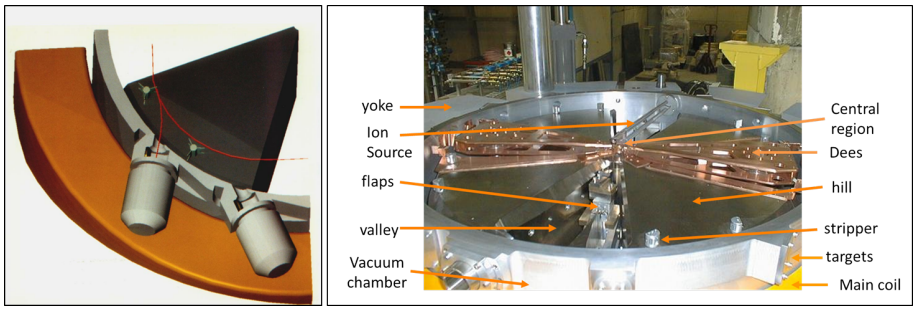

Fig. II.16.17: Left: H^- extraction by stripping. Several targets can be placed around the machine. Right: median plane of a typical IBA isotope production cyclotron, showing the most important subsystems.

4. the ability to place several targets around the machine;
5. simultaneous dual beam extraction;
6. good beam optics.

The energy can easily be varied by moving the radial position of the stripper probe (see Fig. II.16.16). By proper azimuthal positioning of the stripper foil, all orbits come together in the same cross-over point outside the magnetic field. Here, a magnet can be placed that deflects the beam into the beam line. Simultaneous dual beam operation is possible by positioning two stripper foils at an azimuth of 180° with respect to each other. Some fine tuning of the turn-pattern is necessary to distribute the total beam current precisely between the two stripping foils. This may be achieved by adjustment of the dee voltage, or by using first-harmonic coils. Since the extracted beam crosses the radial pole edge at an angle close to 90°, the large (de-)focusing effects of the fringe field are avoided and the beam quality remains intact. H^- stripping is an ideal solution for low- and medium-energy industrial cyclotrons.

There is a serious limitation of an H^- cyclotron, owing to magnetic stripping that may occur during acceleration. Because of this, the magnetic field cannot be high and to obtain high energy the pole radius of the machine must be increased. A well-known example is the TRIUMF cyclotron [23], which accelerates H^- up to 520 MeV. The average magnetic field is only 0.3 T (in the cyclotron centre), resulting in a magnet diameter of 18 m and a magnet weight of 4000 tonnes. The H^- is also stripped on the vacuum rest gas and, to limit beam losses, good vacuum pumping (expensive) and an external ion source is required (IBA Cyclone-IKON, ACS TR30). The H^--cyclotron is good for isotope production, but not for proton therapy.

II.16.4.2 Electrostatic deflector

The ESD creates an outwardly directed DC electric field between two electrodes. The goal is to give an initial angular deflection to the beam. The inner electrode (called the septum) is placed in between the last and penultimate turn. The septum is at ground potential so that the inner orbits in the cyclotron are not affected. At the entrance, the septum is knife-thin (of the order of 0.1 mm) in order to peel off the last orbit and minimize beam losses on the septum itself. To better distribute the heat due to beam losses, the beginning of the septum is often V-shaped. The septum is water-cooled. The heat loss on the septum usually determines the maximum current that can be extracted from the cyclotron. The outer electrode

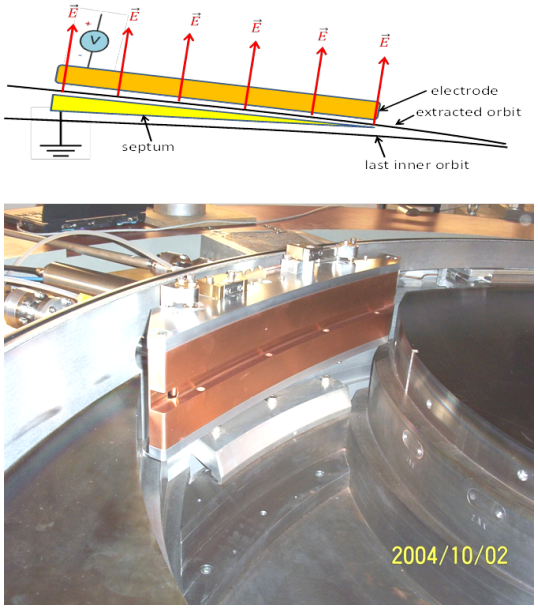

Fig. II.16.18: Top: principle function of an electrostatic deflector. Bottom: electrostatic deflector installed in the IBA C235 cyclotron.

is on a negative potential (assuming extraction of positively charged particles). Of course, the shape of the electrodes must follow the shape of the extracted orbit. Figure II.16.18 illustrates the principle and shows the electrostatic deflector that is used in the IBA C235 cyclotron.

II.16.4.3 Regenerative extraction in the IBA S2C2

In the IBA superconducting synchro-cyclotron (S2C2), extraction with an electrostatic deflector cannot be used, because the turn separation at extraction is far too small. Instead, the regenerative method of extraction based on the $2\nu_r = 2$ resonance is used. The extraction system is fully passive: only soft iron elements are used. The layout is shown in Fig. II.16.19. The regenerator creates a strong magnetic field bump, of which the quadrupole component increases the radial focusing and locks the horizontal betatron frequency ν_r to one. The orbit becomes unstable and is pushed towards the extraction channel by the first-harmonic component of the magnetic field, also produced in the bump. It is essential to avoid the Walkinshaw resonance in this process, as illustrated in Fig. II.16.20. When the extraction sets in, the displacement of the beam towards the extraction channel steadily and exponentially builds up. The magnetic septum of the extraction channel separates the extracted orbit from the last internal orbit. The locking of the betatron frequency ν_r to one can be observed in the left panel of Fig. II.16.20 by the fact that the subsequent azimuth of the nodes of the oscillation is fixed for multiple turns.

A series of iron correction bars compensates the magnetic field undershoots towards inner radii that are produced by the regenerator and the extraction channel. Farther downstream, between the main coils, a three-bar gradient corrector is placed, reducing the radial defocusing in the fringe field of the pole. Finally a permanent magnet quadrupole is used to further match the extracted beam to the external beam line.

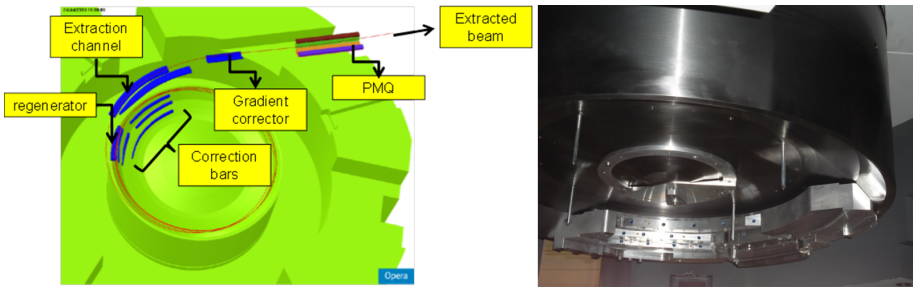

Fig. II.16.19: Passive extraction system of the IBA superconducting synchro-cyclotron S2C2: PMQ, permanent magnet quadrupole.

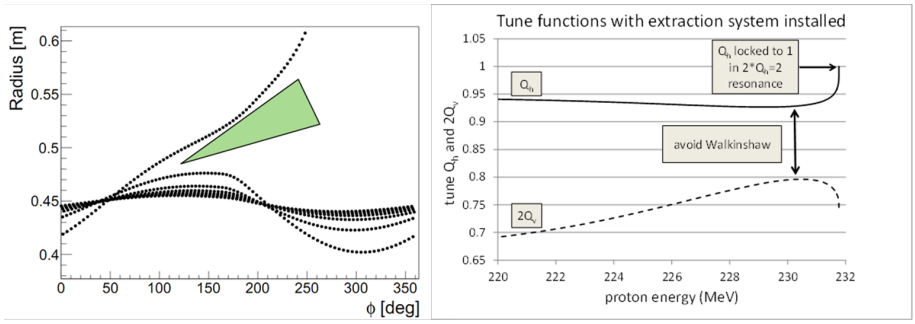

Fig. II.16.20: Regenerative extraction: a strong quadrupole bump increases ν_r and locks it to one. A steady shift of the beam towards the extraction channel is built up. The Walkinshaw resonance ($\nu_r = 2\nu_z$) must be avoided.

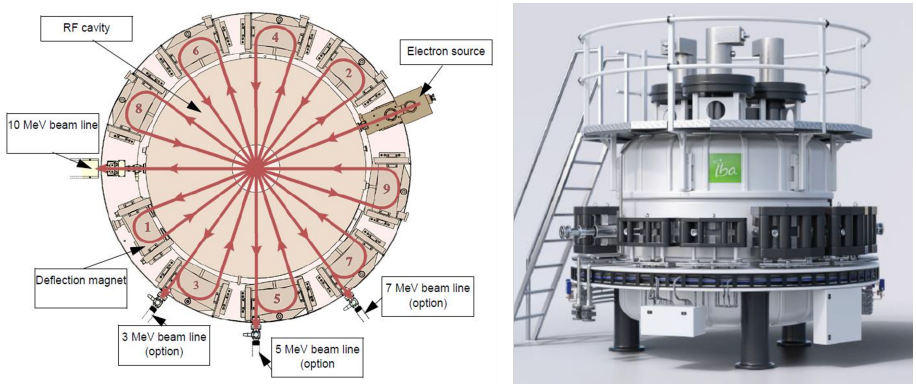

Fig. II.16.21: Left: schematic layout of a rhodotron. Right: the 40 MeV rhodotron.

II.16.5 Rhodotron

Due to the relativistic effect, electrons cannot be accelerated in a cyclotron: an electron with a kinetic energy of 1 MeV for example, is already at 94% of the speed of light. Other means of acceleration are thus needed, such as linear accelerators or so-called Rhodotrons [24].

The Rhodotron is a recirculating accelerator where electrons gain energy by crossing several times a single accelerating cavity (see Fig. II.16.21). This feature makes it possible to operate the machine in a continuous mode. The electrons are generated in a vacuum environment by the source (also called

electron gun), located at the outer wall of the cavity. They are drawn away and accelerated by the radial field, which transmits them its energy. The electrons undergo a first acceleration toward the inner cavity wall. Then, they pass through openings in the center conductor. Since the electric field is reversed when they emerge in the second part of the cavity, electrons are accelerated a second time, completing a crossing of the diameter. An external magnet then bends the accelerated beam and sends it back into the cavity for a second acceleration cycle. The electron beam therefore travels along a rose-shaped path, which explains why the name Rhodotron was chosen.

The Rhodotrons consists of the following major components: an electron gun, a RF power source, the accelerating cavity, the external deflection magnets, a cooling system, and the beam delivery system. At the exit of the accelerator, the beam of high-energy electrons is transported through beam lines from the accelerator to the radiation vault.

Rhodotrons now come in different configurations, with an energy increase of 1 MeV per crossing up to a total of 10 MeV, or for example 3.3 MeV increase per crossing up to a total of 40 MeV. In the latter case there are eleven magnets mounted on the Rhodotron to reinject and, as the RF power is much higher than for a 1 MeV acceleration per crossing, the beam is pulsed: only for 1/8th of the time there is beam, keeping the cooling of the cavity under control. In the TT1000, each time the electrons cross the cavity, their energy increases by 1.2 MeV. Six passes and five magnets give a final 7 MeV beam, at a highest possible intensity of 80 mA, see Ref. [25].

II.16.5.1 Applications

There are multiple applications for high-intensity electron beams. We mention only a few:

1. cargo scanning: expanding the beam in a scan horn on a large target, X-rays can be produced. The large X-ray beam can be used to scan trucks and/or cargo containers at customs;
2. sterilization: one of the major applications for these accelerators is sterilization. Again, producing a large beam of X-rays by scanning the electrons on a target, the X-rays are used to irradiate packages, sterilizing its contents;
3. radio-isotope production: shooting for example on a target creating X-rays, molybdenum-100 (Mo-100) can be transformed into Mo-99. This then serves as generator for technecium-99m (Tc-99m) used in diagnostic nuclear medicine. The use of Rhodotrons for isotope production is new with the first commercial installation under construction (as of 2023).

II.16.5.2 Exercise: cyclotron design

In an excel sheet, build a proton therapy isochronous cyclotron field map, finding a set of parameters such that the field is vertically stable ($\nu_z \sim 0.2 - 0.3$). As hypothesis: 1) the cyclotron is iron dominated; 2) consider hard edge geometry at this early stage of a design. So along each turn, the protons see only B_{hill} or B_{valley}; 3) keep $B_{\text{hill}} < 2.3$ Tesla (which is already very high for an iron dominated cyclotron); 4) keep $B_{\text{hill}} - B_{\text{valley}} < 1.3$ Tesla, which means "deep" valleys; 5) assume 4-fold symmetry.

The free parameters to choose that are constant with the radius are: 1) the angular span of the hills between $45°$–$50°$, keeping enough space for efficient RF cavities; 2) the RF frequency.

The free parameters to choose that are varying with respect to the radius are: 1) the B_{hill} field (and thus also the B_{valley} to keep the field isochronous); 2) the spiral angle. Choose a few values at different radii, and then interpolate between them to have a smooth variation with respect to radius.

The expected outputs are: 1) the chosen B_{hill} and B_{valley} profiles vs radius, from 10 MeV to 230 MeV, thus neglecting the central field; 2) the chosen spiral angle vs radius; 3) ν_z vs radius; 4) a projection in the acceleration plane XY of the hill edges.

For the solution, see https://indico.cern.ch/event/1347740/attachments/2752041/5111806.

References

[1] EuCARD-2, Applications of particle accelerators in Europe (APAE), 2017, doi:10.17181/CERN.HA4I.UT3N.

[2] E.O. Lawrence and M.S. Livingston, *Phys. Rev.* **40** (1932) 19, doi:10.1103/PhysRev.40.19.

[3] V. Veksler, *J. Phys. USSR* **9**(3) (1945) 153.

[4] E.M. McMillan, *Phys. Rev.* **68**(5–6), 143L (1945), doi:10.1103/PhysRev.68.143.

[5] J. Livingood, *Principles of cyclic particle accelerators* (Van Nostrand, New York, 1961), Chap. 6, Internet archive.

[6] L.H. Thomas, *Phys. Rev.* **54** (1938) 580, doi:10.1103/PhysRev.54.580.

[7] https://www.3ds.com/products-services/simulia/products/opera/, last accessed 4 Nov. 2024.

[8] N. Christofilos, Focussing system for ions and electrons, US patent 2736799, priority date 10 March, 1950, Google Patents.

[9] E.D. Courant *et al.*, *Phys. Rev.* **88** (1952) 1190, doi:10.1103/PhysRev.88.1190.

[10] H.L. Hagedoorn and N.F. Verster, *Nucl. Instrum. Meth.* **18–19** (1962) 201, doi:10.1016/S0029-554X(62)80032-9.

[11] P. Heikkinen, Injection and extraction for cyclotrons, in Proc. CERN Accelerator School: 5th General Accelerator Physics Course, Jyväskylä, Finland, 7–18 Sep. 1992, Ed. S. Turner, CERN 94-01 (CERN, Geneva, 1994), pp. 819–839, 10.5170/CERN-1994-001.819.

[12] P. Mandrillon, Injection into cyclotrons, in Proc. CERN Accelerator School: Cyclotrons, Linacs and Their Applications, La Hulpe, Belgium, 28 Apr.–5 May 1994, Ed. S. Turner, CERN 96-02 (CERN, Geneva, 1996), pp. 153–168, doi:10.5170/CERN-1996-002.153.

[13] W. Kleeven, Injection and extraction for cyclotrons, in Proc. CERN Accelerator School: Small accelerators, Zeegse, The Netherlands 24 May–2 Jun. 2005, Ed. D. Brandt, CERN-2006-012 (CERN, Geneva, 2006), pp. 271–296, doi:10.5170/CERN-2006-012.271.

[14] J.-L. Belmont, Ion transport from the source to the first cyclotron orbit, in Proc. XXXIII European Cyclotron Progress Meeting, Warszawa-Kraków, Poland, 17–21 Sep. 2002, *Nukleonika* **48**, supplement 2 (2003), pp. S3–S11, Nukleonika.

[15] W. Kleeven *et al.*, The IBA superconducting synchrocyclotron project S2C2, in Proc. 20th Int. Conf. Cyclotrons and their Applications, Vancouver, Canada, 16–20 Sep. 2013, pp. 115–119, JACoW.

[16] B.F. Gavin, PIG ion sources, in *The physics and technology of ion sources*, 1st ed., Ed. I.G. Brown (Wiley, New York, 1989), pp. 167–185.

[17] J.-L. Belmont and J.L. Pabot, *IEEE Trans. Nucl. Sci.* **13** (1966) 191–193, doi:10.1109/TNS.1966.4324204.

[18] J.-L. Belmont, Axial injection and central region of AVF cyclotrons, in Lecture notes of 1986 RCNP KIKUCHI Summer School on Accelerator Technology, Osaka, Research Center for Nuclear Physics, Osaka, pp. 79–124.

[19] L.W. Root, Design of an inflector for the TRIUMF cyclotron, Ph.D. thesis, University of British Columbia, 1972, doi:10.14288/1.0302432.

[20] R. Baartman and W. Kleeven, *Part. Accel.* **41** (1993) 41–53, Part. Accel..

[21] W. Kleeven and R. Baartman, *Part. Accel.* **41** (1993) 55–70, Part. Accel..

[22] J.I.M. Botman and H.L. Hagedoorn, Extraction from cyclotrons, in Proc. CERN Accelerator School: Cyclotrons, Linacs and Their Applications, La Hulpe, Belgium, 28 Apr.–5 May 1994, Ed. S. Turner, CERN 96-02 (CERN, Geneva, 1996), pp. 169–185, doi:10.5170/CERN-1996-002.169.

[23] G. Dutto, The TRIUMF 520 MeV cyclotron, in Proc. 18th Int. Conf. Cyclotrons and their Applications, Vancouver, Canada, 6–10 Jul. 1992, Eds. G. Dutto and M.K. Craddock (World Scientific, 1993), pp. 138–142, JACoW.

[24] J. Pottier, *Nucl. Instrum. Meth. Phys. Res*$\dot{B}$ **40–41** (1989) 943, doi:10.1016/0168-583X(89)90512-0.

[25] M. Abs *et al.*, *Radiat. Phys. Chem.* **71**(2004) 287, doi:10.1016/j.radphyschem.2004.03.061.